Journal of Inflammation Research

Dovepress
Taylor & Francis Group

Open Access Full Text Article

ORIGINAL RESEARCH

Exploring the Potential of Coix Seeds to Mitigate High Humidity-Induced Gut Inflammation via Microbiota and Metabolite Modulation

Peihan Zhao[1], Congyou Xiao[1], Mingyang Xuan[1], Shuxin Yan[1], Xue Yu[2], Wei Li[1], Linxiao Han[1], Hanxi Wang[1], Jingbo Zhao[1], Shujing Zhang[2], Xianggen Zhong[1]

[1]Institute of Synopsis of Golden Chamber Department, School of Traditional Chinese Medicine, Beijing University of Chinese Medicine, Beijing, People's Republic of China; [2]Experimental Center, School of Traditional Chinese Medicine, Beijing University of Chinese Medicine, Beijing, People's Republic of China

Correspondence: Xianggen Zhong; Shujing Zhang, School of Traditional Chinese Medicine, Beijing University of Chinese Medicine, Northeast Corner of the Intersection of Yangguang South Street and Baiyang East Road, Liangxiang University Park, Fangshan District, Beijing, 102401, People's Republic of China, Email zhongxg@bucm.edu.cn; Jingshuzhang@126.com

Background: Extreme humidity exacerbates gastrointestinal disorders by disrupting gut microbiota homeostasis, compromising the intestinal barrier and triggering immune dysregulation. Coix seed (*Coix lacryma-jobi* L.), widely used in traditional Chinese medicine for eliminating dampness, shows promise; however, its mechanisms require further elucidation.

Methods: A Coix seed decoction (CD) was administered to rats exposed to 85% relative humidity (8 h/day) for 30 days. Forty rats were randomly divided into four groups: control, high-humidity exposed, Coix seed-treated control and Coix seed-treated high-humidity. The chemical composition of the CD was characterised using ultra-high-performance liquid chromatography–mass spectrometry (LC-MS), and faecal moisture content, body weight and histopathological changes were assessed. Colonic tissues were analysed by haematoxylin–eosin staining and transmission electron microscopy for structural integrity. Gut microbiota were profiled using 16S ribosomal RNA sequencing, followed by bioinformatic analysis of diversity, differential abundance and co-occurrence networks. Untargeted metabolomics was performed using LC-MS to identify metabolic alterations, and the serum inflammatory cytokines (tumour necrosis factor alpha [TNF-α], interleukin [IL]-6, IL-17) were measured by enzyme-linked immunosorbent assay.

Results: High humidity disrupts gut homeostasis in rats by inducing intestinal damage, inflammation, dysbiosis and lipid metabolic disorders. Coix seed decoction significantly alleviated these effects, restoring colonic structure, rebalancing the gut microbiota (eg increasing *Erysipelatoclostridium* spp. *Akkermansia* spp. *Lactobacillus* spp. and reducing *Escherichia* spp. *Shigella* spp.) and correcting sphingolipid metabolism (eg sphingomyelin, ceramide). Metabolomic and transcriptomic analyses revealed that CD suppressed immune-related pathways (eg T/B cell receptor signalling, Th1/Th2 differentiation), consistent with reduced serum levels of proinflammatory cytokines (TNF-α, IL-6, IL-17). Correlation networks highlighted interactions between key microbes and metabolites, suggesting a regulatory role for *Ruminococcus* spp., *NK4A214_group* spp. and *Prevotellaceae NK3B31* spp. in the therapeutic effects of CD.

Conclusion: Our findings provide experimental evidence that Coix seed mitigates high humidity-induced gut injury through microbiota remodelling, lipid metabolic regulation and immune modulation.

Keywords: coix seed, humidity, metabolomics analysis, gut microbiota, 16S ribosomal ribonucleic acid sequencing

Introduction

As global warming intensifies, episodes of extreme humidity and heat have become increasingly frequent, contributing to a rise in climate-related diseases. Over the past 4 years, the duration of extreme humidity events has dramatically increased, particularly in subtropical regions, potentially exacerbating the emergence and spread of climate-related epidemics.[1,2] The World Health Organization projects that climate change-related health impacts could result in approximately 250,000 annual fatalities attributable to nutritional deficiencies and diarrhoeal diseases during the

Received: 17 March 2025
Accepted: 21 July 2025
Published: 30 July 2025

2030–2050 period, with projected direct health-care costs being USD 2–4 billion annually.[3] High humidity also facilitates the transmission of infectious agents, with projections indicating a 10% increase in diarrhoeal disease incidence among children by 2030.[4] In light of these significant public health challenges, the role of ambient humidity as a modifiable environmental factor influencing the pathogenesis and progression of gastrointestinal disorders has garnered increasing scientific attention.[5]

Extreme humidity has been shown to disrupt the gut microbiome, compromise the intestinal mucosal barrier,[6] alter the immune response[7] and potentially affect mental health outcomes.[8] Although supplementation with *Lactobacillus murinus* has demonstrated potential in restoring gut dysbiosis induced by humid-heat environments, its safety and long-term efficacy in real-world settings remain to be fully established.[8] Therefore, there is an urgent need for comprehensive research into the effects of climate variability on intestinal microbiota homeostasis and systemic health, alongside the development of evidence-based therapeutic strategies to mitigate these environmental health risks.

Coix seed (*Coix lachryma-jobi* L.), a traditional medicinal herb and functional food in traditional Chinese medicine (TCM), has been historically employed for dampness elimination and gastrointestinal regulation, as documented in ancient pharmacopoeias such as Shennong's Classic of Materia Medica (Han Dynasty) and the Treatise on Typhoid and Miscellaneous Diseases. Modern pharmacological studies have elucidated its multifaceted bioactivities, including modulation of gut microbiota, immunoregulatory effects and anti-inflammatory properties. Specifically, clinical evidence suggests that Coix seed supplementation can significantly enhance gut microbial diversity and improve immune function in healthy individuals.[9] Moreover, its ethanol-extractable fractions – rich in phenolic and flavonoids – exhibit potent anti-inflammatory and antitumor activities.[10,11] Notably, the high dietary fibre content of Coix seed supports gut health by promoting probiotic growth, enhancing vitamin biosynthesis and modulating immune response.[12–14] These properties position Coix seed as a promising nutraceutical intervention for mitigating climate change-associated gastrointestinal disturbances and advancing global nutritional health initiatives.

In this context, we conducted an integrated multi-omics investigation – including gut microbiome profiling and untargeted metabolomics – to evaluate the protective effects of Coix seed against high humidity-induced gut dysfunction. Our results provide mechanistic insights into how Coix seed may alleviate humidity-associated intestinal inflammation through microbiota remodelling and metabolic regulation, offering a potential dietary strategy to address climate-related health risks.

Materials and Methods

Animals and Groups

Male Sprague–Dawley rats (body weight 400 ± 10 g) were sourced from SPF Laboratory Animal Technology Co., Ltd. (China; License No. SYXK [Jing] 2023–0011) and acclimatised in a specific pathogen-free barrier environment at the Beijing University of Chinese Medicine. The animals were maintained under controlled environmental conditions (21°C–24°C, 40–60% relative humidity) and a standardised photoperiod (12 h light/12 h dark). All animals received unrestricted access to sterilised drinking water and commercial rodent feed during the study. The experimental protocols strictly followed the ethical guidelines authorised by the Institutional Animal Ethics Committee of Beijing University of Chinese Medicine (Protocol ID: BUCM-2023090503-3117).

To assess the impact of elevated humidity on gut health in animal models, 20 rats were stratified via random number assignment into two groups: a baseline control group (CON) and a high-humidity exposure group (HH). In a parallel experiment evaluating the dampness-dispelling effects of Coix seed, another 20 rats were similarly randomised into a Coix seed decoction (CD)-treated control group (CD-CON) and a CD-administered HH group (CD-HH).

Drugs and Reagents

The Coix seeds utilised in this research were commercially sourced from Beijing Tongrentang Pharmaceutical Co., Ltd. (Beijing, China). Biochemical analysis reagents, including enzyme-linked immunosorbent assay (ELISA) detection kits, were supplied by Beijing Bioway Co., Ltd. (Beijing, China).

Drug Preparation

The CD was prepared following established protocols. Briefly, raw Coix seeds underwent hydration in 10× volume of double-distilled water (30 min), followed by sequential thermal processing: intense boiling (100°C) and subsequent low-heat simmering (40 min). Post-extraction, the solution was replenished with additional solvent (30 min), vacuum-filtered and vacuum-concentrated to achieve a final concentration of 1 g crude botanical mass per millilitre. Pharmacological equivalence was determined through allometric scaling from human clinical doses (Chinese Pharmacopoeia, 2010 Edition), yielding a calculated rat-equivalent dosage of 6.25 $g \cdot kg^{-1} \cdot d^{-1}$.[15]

Ultra-High-Performance Liquid Chromatography–Mass Spectrometry-Based Phytochemical Profiling of Coix Seed Decoction

The chemical composition of the CD was characterised using ultra-high-performance liquid chromatography-mass spectrometry (UHPLC-MS). Prior to analysis, sample pretreatment involved sequential processing: initial centrifugation (12,000 rpm, 12 min) to isolate the bioactive fraction, followed by methanol extraction with vortex homogenisation (3,000 rpm, 90s) and ultrasonication (5 min). Post-incubation stabilisation at 4°C (20 min) preceded secondary centrifugation (12,000 rpm, 15 min). The resulting supernatant underwent microfiltration (0.22 μm membrane) prior to chromatographic analysis.

Chromatographic separation was achieved on a Vanquish Ultra HPLC system (Thermo Scientific, USA) using a Waters Acquity UPLC HSS T3 column (2.1 × 100 mm, 1.8 μm). The binary mobile phase comprised the following:

- Eluent A: Ultrapure water + 0.1% formic acid
- Eluent B: Acetonitrile + 0.1% formic acid

A multistep gradient programme was implemented as follows:
0–3 min: 5% B (isocratic)
3–35 min: 5% → 60% B (linear gradient)
35–45 min: 60% → 98% B (steep gradient)
45–46 min: 98% → 5% B (rapid equilibration)
46–50 min: 5% B (column reconditioning)
Operational parameters included the following:

- Flow rate: 0.3 $mL \cdot min^{-1}$
- Column temperature: 35°C
- Injection volume: 5 μL
- Dual ion mode detection (positive/negative electrospray ionisation [ESI])

Experimental Procedures

Following established protocols from prior research,[7] the experimental groups underwent differential interventions, as follows:

- Environmental exposure: The HH and CD-HH cohorts were subjected to 8-h daily sessions in a controlled climatic simulation chamber.
- Pharmacological intervention: The CD and CD-HH groups received a single daily oral gavage of CD.
- Control treatment: The CON and HH-CON groups were administered equivalent volumes of sterile distilled water (see Table 1 for experimental design).

Gravimetric monitoring was conducted weekly to track physiological changes across cohorts.

Table 1 General Information of Experimental Design

Group	Animal	Quantity	Sex	Temperature (°C)	Humidity (%)	Intervention (6.25g/kg/d)	Faecel Moisture (%)
CON	Rat	10	Male	21-24	50 ± 5, 24h	Distilled water	62.4 ± 4.5
HH	Rat	10	Male	21-24	80 ± 5, 8h, 50 ± 5, 16h	Distilled water	65.8 ± 3.5
CD-CON	Rat	10	Male	21-24	50 ± 5, 24h	Coix seed decoction	58.4 ± 3.5
CD-HH	Rat	10	Male	21-24	80 ± 5, 8h, 50 ± 5, 16h	Coix seed decoction	60.5 ± 7.4

Sample Collection

Similar to a previous study, the mice showed physiological symptoms such as diarrhoea and weight loss after 15 days of improper diet and a high-humidity environment.[16] At the experimental endpoint (day 30) in this study, two faecal specimens were collected per rat for moisture content analysis. Faecal moisture quantification was performed via gravimetric analysis: ([pre-desiccation mass−post-desiccation mass]/pre-desiccation mass) × 100%. Additional faecal samples were immediately snap-frozen in liquid nitrogen and stored at −80 °C for subsequent gut microbiome profiling. For euthanasia, rats were anesthetized with sodium pentobarbital and blood was collected from the abdominal aorta. Colonic tissues were rapidly excised using sterile techniques and prepared for histopathological and ultrastructural analyses.

Histopathological and Ultrastructural Analysis

For the histopathological examination, colonic specimens underwent a standardised histoprocessing workflow: chemical immobilisation (4% paraformaldehyde), ethanol dehydration series, paraffin-embedded block preparation, microtome sectioned at 3 μm thickness and haematoxylin–eosin chromatic labelling. Digital histomorphometry was performed using the ASAP platform (v2.2.0) to quantify architectural alterations.

For the ultrastructural analysis, additional tissue samples were processed through ultrastructural characterisation protocols: glutaraldehyde immobilisation, graded solvent dehydration, epoxy resin embedding, ultrathin sectioning (60–80 nm), uranyl acetate-lead citrate dual staining and nanoscale visualisation via transmission electron microscopy (TEM). A blinded evaluation approach was used, in which an independent pathologist scored the samples without knowledge of their group assignments. The histopathological scoring system evaluated four parameters: (1) epithelial damage (0 – no injury, intact epithelium; 1 – mild damage, minimal cell shedding; 2 – moderate damage, partial loss of epithelium; 3 – severe damage, extensive epithelial loss), (2) microvillus status (0 – normal, neatly arranged microvilli; 1 – mild disorganisation or reduction; 2 – significant reduction or shedding; 3 – widespread loss, nearly absent), (3) tight junction integrity (0 – normal gaps, clear structure; 1 – mild widening; 2 – marked widening affecting barrier function; 3 – extreme widening, severely impaired integrity) and (4) mitochondrial morphology (0 – normal size and cristae, 1 – mild swelling, few abnormal mitochondria; 2 – noticeable swelling, many altered mitochondria; 3 – severe swelling, structural destruction). All the image captures were obtained under the same parameters.

16S Ribosomal Ribonucleic Acid Gene Sequencing

Extraction and Library Construction

Genomic DNA was purified from faecal samples using the MagPure Soil DNA LQ Kit (Magan Biotech, China), followed by library preparation and 16S ribosomal RNA (rRNA) hypervariable region sequencing (V3-V4) conducted by OE Biotech Co., Ltd. (Shanghai, China) using universal primers 341F (5′-CCTAYGGGRBGCASCAG-3′) and 806R (5′-GGACTACNNGGGTATCTAAT-3′). Taxonomic profiling of gut microbiota was performed through alignment and preliminary annotation using the SILVA database, and the functional metabolic potential was inferred via PICRUSt2-based Kyoto Encyclopedia of Genes and Genomes (KEGG) pathway annotation.

Gut Microbiome Bioinformatic Workflow

Initial sequencing outputs (in FASTQ format) underwent quality control, including adapter trimming via Cutadapt (v3.4). Chimaera removal and denoising were executed through the DADA2 algorithm within the QIIME2 pipeline (v2020.11), generating a non-redundant amplicon sequence variant (ASV) feature table Taxonomic annotation of ASVs was conducted using the SILVA 138 reference database within the QIIME2 pipeline.

To assess the α diversity of the gut microbiota, multiple metrics and methods were employed. First, Faith's phylogenetic diversity (PD) index (PD whole tree) was calculated, an index based on the phylogenetic tree that reflects the evolutionary relationships among species. Additionally, rank-abundance curves were generated to visually display the relative abundance distribution of ASVs across different groups. Beta (β) diversity metrics were derived through principal coordinate analysis (PCoA) employing unweighted UniFrac dissimilarity matrices computed using the "phyloseq" R package (v1.34.0). A Permutational Multivariate Analysis of Variance (PERMANOVA) was conducted to examine inter-group variations in β diversity and Inter-group taxonomic disparities were assessed via one-way analysis of variance (ANOVA) implemented in the "vegan" R package (v2.6–4), followed by linear discriminant analysis effect size (LEfSe) modelling to identify differentially abundant taxa (linear discriminant analysis score > 2.0). Co-occurrence network topology was reconstructed using SparCC correlation coefficients ($|\rho| > 0.3$, $p < 0.01$), visualised through Gephi (v0.9.7) with force-directed layout algorithms.

Metabolomic Analysis

Extraction of Metabolites and Quality Control

Cryopreserved biospecimens (−80°C) underwent controlled thawing via ice–water immersion to mitigate metabolite degradation. Aliquots (200 μL) were transferred to pre-chilled 1.5 mL microcentrifuge tubes, followed by precipitation with 100 μL of chilled methanol–acetonitrile solvent (2:1 v/v). Homogenisation involved sequential vortex agitation (1 min, 2,500 rpm) and ice-bath ultrasonication (40 kHz, 10 min), succeeded by phase separation through cryogenic incubation (−40°C, 12 h). Post-precipitation clarification was achieved via refrigerated centrifugation (4°C, 12,000 × g, 10 min).

Supernatant fractions (150 μL) were aspirated using pre-cooled glass syringes, subjected to 0.22 μm membrane microfiltration and aliquoted into LC-MS-certified vials in an inert atmosphere. Processed samples were cryostored (−80°C) until liquid chromatography–mass spectrometry (LC-MS) profiling. Quality assurance included interspersed pooled quality control samples generated through equimolar blending of all study specimens. Raw spectral data processing and metabolite annotation were conducted by Shanghai Luming Biotech (China) using proprietary Compound Discoverer™ workflows.

Untargeted Metabolite Profiling

Untargeted metabolomic profiling and serum samples obtained from the four groups were analysed via LC-MS. The equipment used included an Acquity UPLC I-Class Plus system (Waters Corporation, Milford, USA) connected to a Q-Exactive mass spectrometer with a heated ESI source (Thermo Fisher Scientific, Waltham, MA, USA). The ESI was conducted in both positive and negative ionisation modes for metabolite profiling.

Metabolite Annotation and Inference

Raw LC-MS spectra underwent multistep preprocessing via Progenesis QI (v2.3, Waters Corporation), including baseline correction, chromatographic peak deconvolution, retention time alignment and intensity normalisation. Metabolite annotation leveraged high-resolution mass accuracy (<5 ppm), MS/MS fragmentation patterns and isotopic signatures through cross-referencing against The Human Metabolome Database (2023), LipidMAPS (v2.3), METLIN and in-house spectral libraries.

Multivariate statistical modelling was implemented in R (v4.2.1), as follows:

1. Exploratory analysis: Principal component analysis evaluated global metabolic variance and analytical batch consistency.

2. Supervised modelling: Orthogonal partial least squares–discriminant analysis (OPLS-DA) identified intergroup discriminative metabolites, with variable importance in projection (VIP) scores quantifying feature contribution to class separation.
3. Hypothesis testing: Two-tailed *t*-tests (false discovery rate-corrected) validated differential metabolites (VIP > 1.0, $p < 0.05$).

Significantly altered metabolites underwent KEGG pathway enrichment analysis (https://www.kegg.jp) to elucidate perturbed biochemical networks.

Enzyme-Linked Immunosorbent Assay Analysis

Serum concentrations of proinflammatory cytokines (tumour necrosis factor alpha [TNF-α], interleukin [IL]-6, IL-17) were quantified via sandwich ELISA following manufacturer protocols. Optical density measurements at 450 nm were acquired using a Varioskan LUX multimode microplate reader (Thermo Fisher Scientific), with wavelength calibration performed against reference blanks prior to sample analysis.

Statistical Analysis

Quantitative results are expressed as mean ± standard error of the mean. Statistical comparisons were performed using one-way ANOVA for multigroup analyses, with post hoc pairwise contrasts assessed via unpaired Student's *t*-tests. Data visualisation and computational modelling were executed through GraphPad Prism (v8.0, San Diego, CA) and the Metware Cloud metabolomics suite (www.metware.cn), respectively. The significance threshold was established at $p < 0.05$ for all inferential analyses.

Results

Ultra-High-Performance Liquid Chromatography – Mass Spectrometry Analysis of the Coix Seed Decoction

The phytochemical composition of the CD was systematically characterised via UHPLC-MS. Figure 1 illustrates the representative base peak chromatogram derived from the CD analysis. Chromatographic elution profiles combined with high-resolution mass spectral data enabled the detection of nine bioactive constituents, as catalogued in Supplementary Table 1.

High-Humidity Environment-Induced Colon Pathology Damage and Inflammation Infiltration

In this experiment, rats on the high-humidity diet (the HH group) became inactive, ate less, had messy fur, diarrhoea and lost weight. Rats in the CON and Coix seed-control (CD-CON) groups showed the opposite trends. Figure 2A tracks

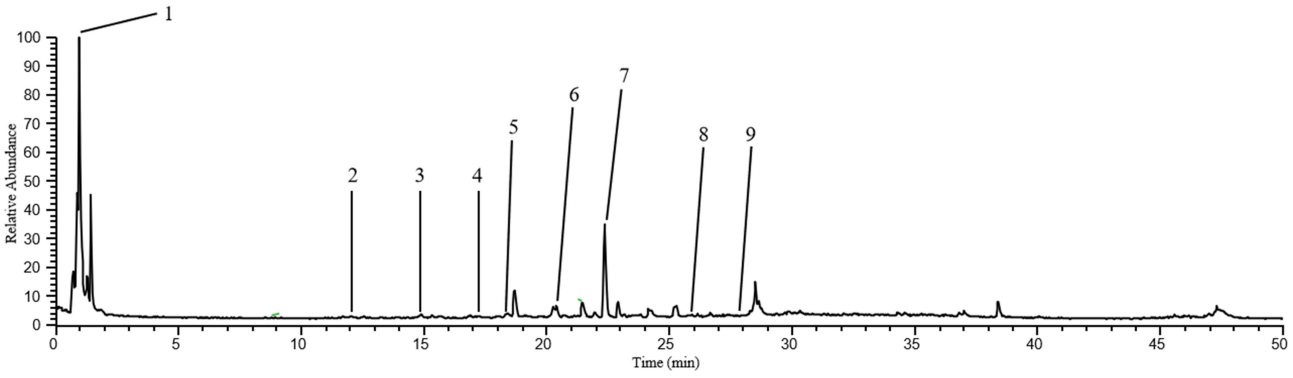

Figure 1 UHPLC-MS analysis of CD.

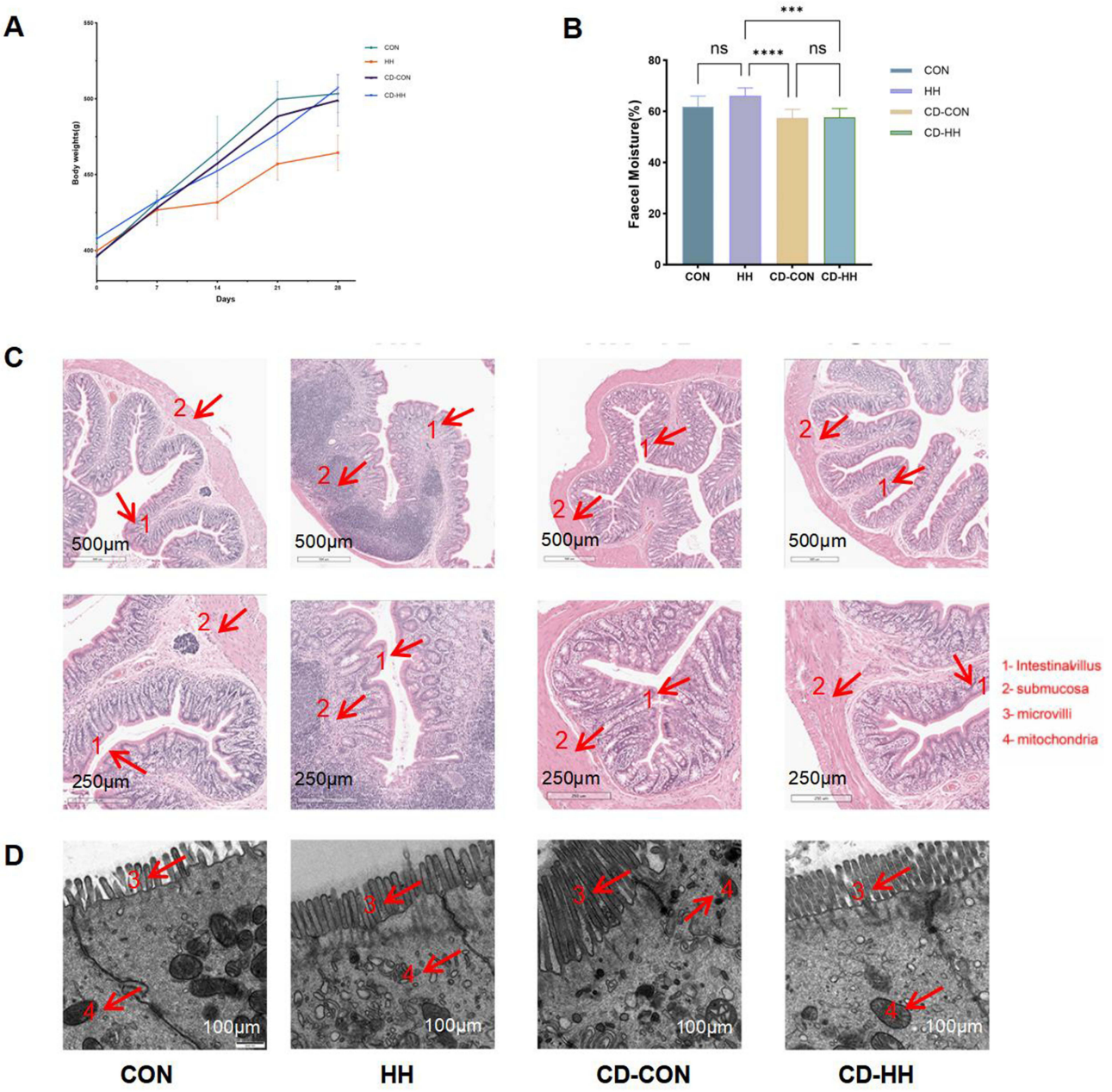

Figure 2 High humidity environment induced colon pathology damage and inflammation infiltration. (**A**) Changes in body weight; (**B**) Changes in faecal moisture content; (**C**) Microscopic images of stained colon of rats; and (**D**) TEM images showing the morphology and structure of colonic cells. (ns is no significance, ***p < 0.001, ****p < 0.0001).

body weight changes. The HH group's weight dipped slightly versus the CON group, whereas the Coix seed-treated high-humidity diet group (CD-HH) showed a rising trend; this may be due to spleen deficiency caused by high-humidity exposure, which leads to reduced diet and weight loss in mice, and the Coix seed can improve the health of mice in high-humidity conditions. Figure 2B shows that the HH group's faecal moisture was much higher than the CON group's, and the CD-HH group's was lower than the HH group's. Haematoxylin-eosin staining further indicated that the HH group exhibited significant pathological changes such as shortened, fused, or shed villi, swollen, necrotic, or exfoliated epithelial cells, along with inflammatory cell infiltration in the lamina propria and edema in the submucosa compared with the CON group, while Coix seed treatment improved the above pathological changes, resulting in a more intact villus structure, better-organized epithelial arrangement, and reduced inflammation (Figure 2C). The TEM showed that the morphology and structure of colonic cells were intact in the CON and CD-CON groups, with neatly arranged

https://doi.org/10.2147/JIR.S524947

microvilli, a clear and intact colonic epithelial barrier and abundant uniformly sized mitochondria. In contrast, the HH group exhibited shedding and loss of colonic microvilli, significant widening of tight junctions, swollen mitochondria and structural defects in mitochondrial cristae (Figure 2D). Histological analysis showed that the CON and CD-CON groups had normal tissue structure, with all parameters scoring 0. The HH group exhibited considerable damage, including epithelial injury, microvillar loss, widened tight junctions and mitochondrial swelling, with scores of 2. The CD-HH group showed mild injury, which was less severe than that in the HH group, with all parameters scored as 1 (Table S2). Although the colonic barrier structure was repaired in the CD-HH group, some microvilli were still absent, and the number of mitochondria increased.

Coix Seed Reversed the Microbiome Dysbiosis Under High Humidity

In the authors' previous study, HH exposure induced dysbiosis of the intestinal microbiome and intestinal inflammation.[7] However, further investigations are needed to understand how Coix seeds reverse these effects under HH conditions. In this study, the effect of Coix seeds on gut dysbiosis caused by a high-humidity diet was analysed by 16S rRNA gene sequencing of microbial DNA from faecal samples. A Venn diagram showed that all four groups shared 40 ASVs. The HH and CON groups shared 349 ASVs, and the CD-HH and HH groups shared 382 (Figure 3A). Analysis of the top three phyla (Figure 3B) found that the HH group had fewer ASVs than the CON group, with Proteobacteria being the most common phylum in the HH group. Phylogenetic diversity whole tree is a metric used to assess microbial community diversity, with higher values indicating greater diversity. As shown in Figure 3C of α-diversity, the CON group exhibited a steady increase in PD whole tree values with sequencing depth, eventually reaching a plateau, which reflects a rich and stable microbial community. In contrast, the HH group showed consistently lower PD whole tree values than the CON group across all sequencing depths, indicating that high humidity negatively impacted microbial diversity. The CD-CON group displayed PD whole tree values similar to those of the CON group, suggesting that the CD did not significantly alter microbial diversity. Notably, the CD-HH group had higher PD whole tree values than the HH group and was closer to the levels observed in the CON and CD-CON groups, indicating that the control diet partially mitigated the adverse effects of high humidity on microbial diversity. Figure 3D illustrates the relative abundance trends of ASVs across ranks in different groups. In the CON group, ASV abundance declined sharply with increasing rank, indicating dominance by a few ASVs. In contrast, the HH group showed a flatter curve, reflecting a more even distribution and structural changes due to high humidity. The CD-CON group was similar to CON, showing no significant effect of the control treatment. The CD-HH group fell between HH and CON, suggesting that the control treatment partially reversed the microbial community changes caused by high humidity. In addition, α-diversity analysis revealed differences in microbial community richness and evenness among different groups, Coix seed treatment significantly improved the diversity of the gut microbiota in HH group at the α-diversity level, bringing it partially back to a level close to that of the CON group (Figure 3E). In contrast, β-diversity analysis highlighted compositional dissimilarities between sample groups with a clear separation observed between the HH and CON groups, CD-HH group exhibited some shifts in microbial community structure compared to the HH group, it did not completely return to the position of the CON group. Moreover, the CON group appeared "dislocated" in space relative to the other groups, indicating that the primary effect of Coix seed lies in enhancing microbial diversity rather than fully restoring the microbial community structure (Figure 3F). The results of the PCoA illustrated the differences between sample groups, showing that all four groups were distinctly separated based on Bray–Curtis operational taxonomic units.

The HH group exhibited a higher abundance of Proteobacteria and an elevated ratio of Bacteroidetes/Firmicutes, whereas the CD-HH group showed the opposite trend (Figure 4A). At the genus level, the HH group saw a marked rise in *Escherichia-Shigella, Lachnospiraceae_NK4A136*_group and *Bacteroides* and a drop in *Lactobacillus, Prevotellaceae_NK3B31_group* and *Alloprevotella. Coix* seed intake altered these genera's abundance ratios (Figure 4B). The heatmap indicated the HH environment specifically upped *Akkermansia* spp. and *Erysipelatoclostridium* spp. levels (Figure 4C). The LEfSe analysis uncovered microbial differences across the four groups. Notably, Coix seed intervention reversed the HH-induced shifts in *Erysipelatoclostridium* spp. and *Akkermansia* spp. distributions. In contrast, the CD-CON group witnessed increased *Prevotellaceae NK3B31* group spp., *Roseburia* spp., *Eubacterium xylanophilum* spp. and *Monoglobus* spp. (Figure 4D). The abundance of *Akkermansia* spp. and *Erysipelatoclostridium* spp. in the four groups

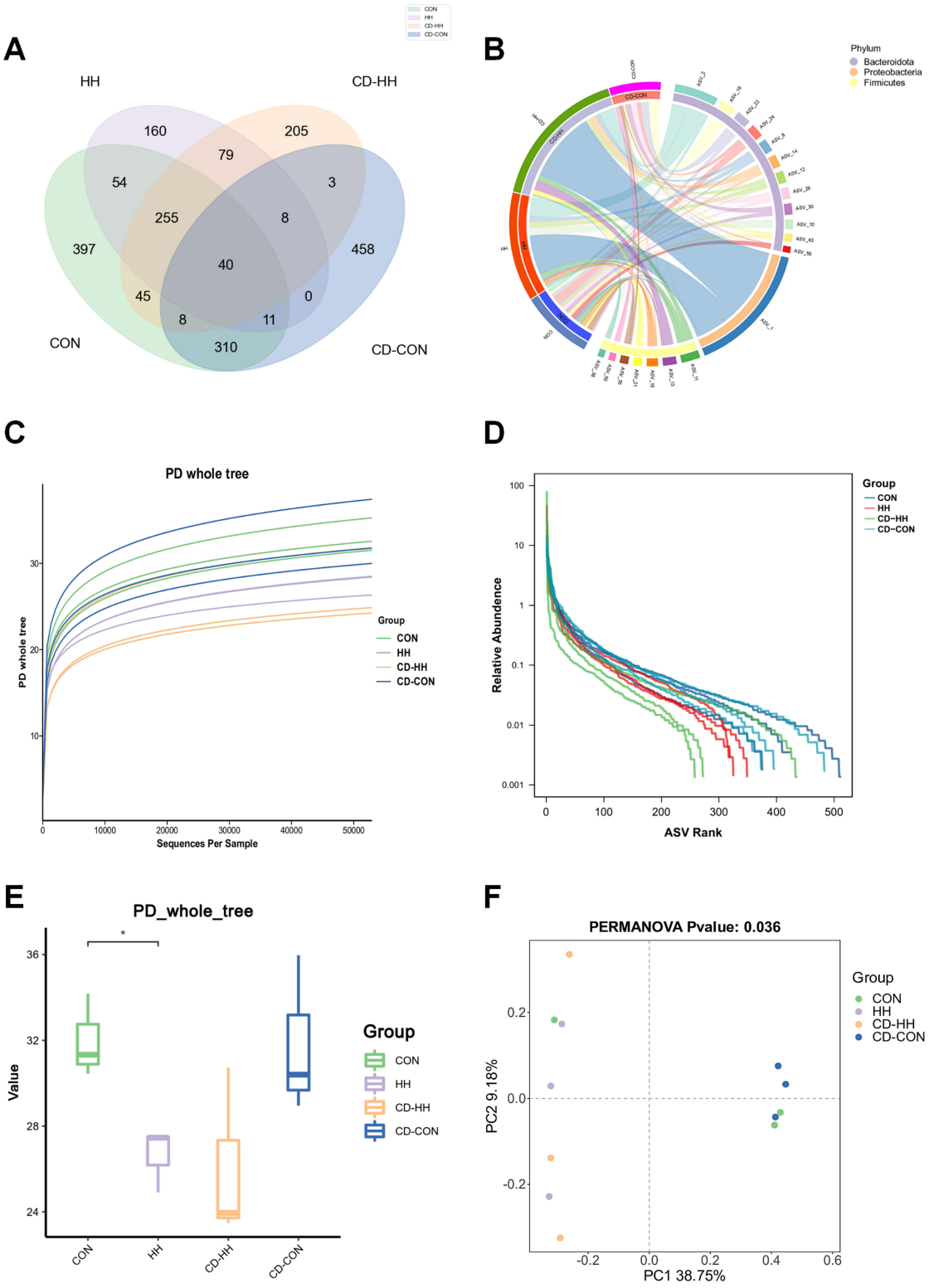

Figure 3 The results of microbial community diversity analysis of gut microbiota: (**A**) Venn diagram; (**B**) Circos sample-species relationship chart of the top 20 most abundant ASVs in each group. The outer circles represent the grouping information, the inner circles represent the relative abundance of the species, and the line connecting the species to the samples represents the distribution of the species, where the thickness of the line is proportional to the abundance; (**C**) Rarefaction curves showing the average PD whole tree number for three groups; (**D**) Rank Abundance curves showing the abundance and homogeneity of samples in each group; (**E**) Results of α-diversity (PD_whole tree) analysis. Data are presented as mean ± standard deviation (SD), with *p < 0.05; (**F**) Results of PCoA analysis.

https://doi.org/10.2147/JIR.S524947

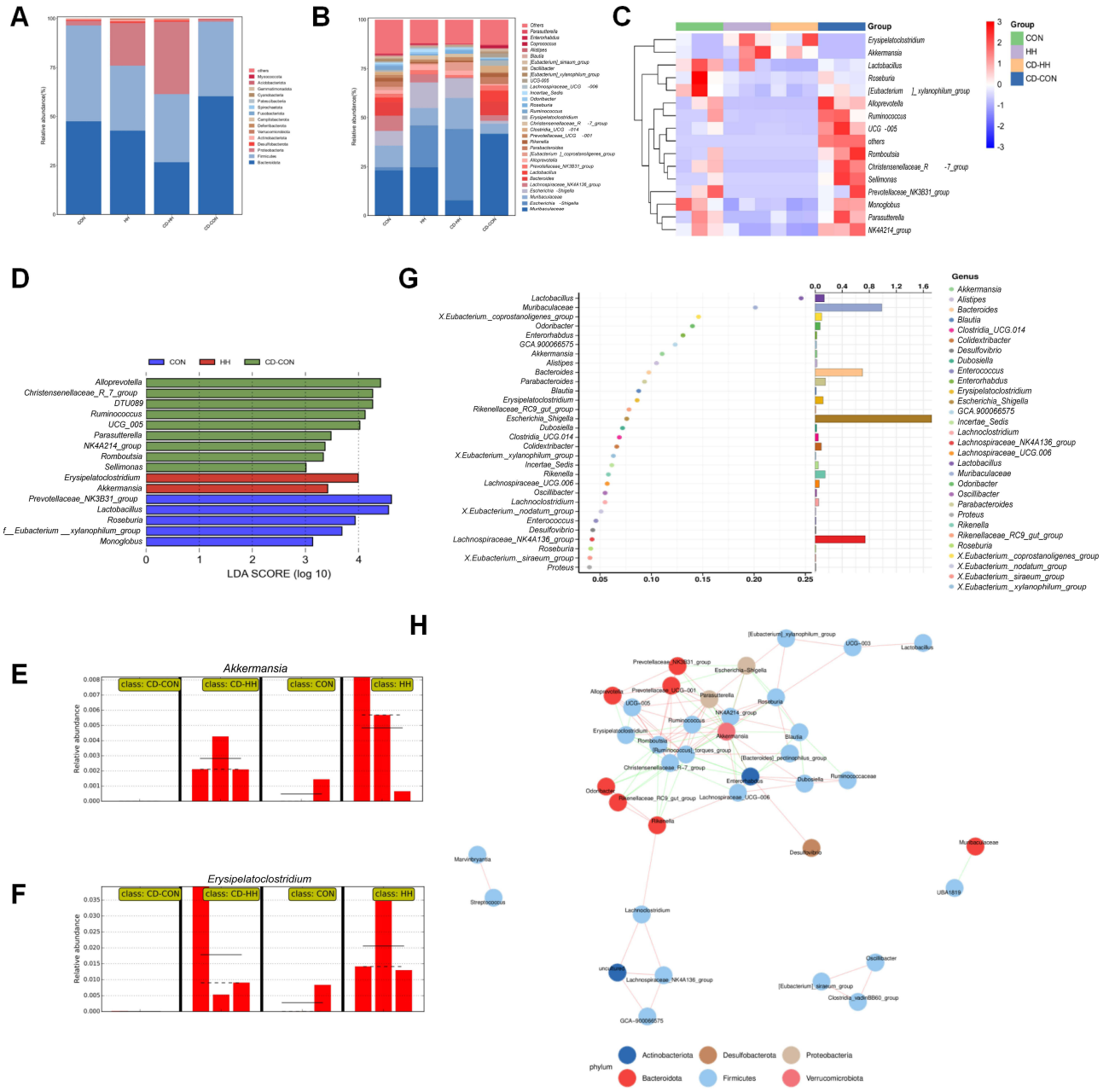

Figure 4 Coix seed reversed the intestinal dysbiosis induced by HH environment. (**A** and **B**) Microbial abundance at the phylum and genus level; (**C**) Heatmap of microbial species at the genus level; (**D**) Results of LEfSe analysis; (**E** and **F**) Histogram showing relative abundance data of gut microbiota, where the solid line represents the mean value and the dashed line shows the median value of relative abundance. (**G**) Random forest plot; and (**H**) Relevance network diagram. Spearman correlation coefficients were calculated based on relative abundance, illustrating the interrelationships of microbial species.

was then analysed (Figure 4E and F); the relative abundance of *Akkermansia* was significantly increased under high-humidity conditions (HH group). The CD treatment helped maintain a relatively stable abundance of *Akkermansia*, especially in the CD-HH group, where its level was similar to that in the CD-CON group. For *Erysipelatoclostridium*, its relative abundance significantly increased in the HH group under high humidity. Under high-humidity conditions, the CD further elevated the abundance of *Erysipelatoclostridium* in the CD-HH group, reaching levels much higher than those in the other groups. Furthermore, the random forest algorithm was used to classify the microbial community samples and identify the key genera in different groups (Figure 4G). Intercolonial interactions (Figure 4H) revealed broad inhibitory effects of *Akkermansia* spp. on *Roseburia* spp., *Eubacterium xylanophilum* spp., *Ruminococcus* spp. and *Prevotellaceae NK3B31* spp.

Coix Seed-Mediated Dysbiosis of Lipid Metabolism Under High Humidity

In total, 3,530 metabolites were identified by comparing the generated substances with those in the metabolomic database. Among these, 1,292 metabolites were identified as lipids (Figure 5A). Principal component analysis and OPLS-DA (Figure 5B–D) separated the HH and CON groups distinctly, and the values of $R^2Y > 0.8$ and $Q^2Y > 0.5$ in OPLS-DA analysis showed good model validity and predictive ability. The metabolites in the HH group and the CON group showed a significant separation trend, indicating that high humidity altered the metabolic profile of normal rats, whereas the metabolic features of the CD-HH group and the HH group exhibited significant differences, suggesting that the intake of Coix seeds changed the levels of metabolites under high humidity conditions. Volcano plots (Figure 5E–G) were used to show variable metabolites among groups. There were 110 differential metabolites in HH versus CON, 51 in CD-HH versus HH and 84 in CD-CON versus CON. These results emphasise the metabolic changes due to high humidity and the corrective impact of Coix seed intervention. High humidity disrupted lipid and organic acid metabolism, upregulating related metabolites; however, Coix seed intervention reversed these changes (Table 2).

To show sample relationships and metabolite expression differences, hierarchical clustering was performed for all significantly different metabolites and the top 50 based on VIP score (Figure 6A and B). This indicated that CD intervention under humidity improved sphingomyelin (SM), ceramide (Cer), phosphatidylserine and Nigelic acid levels. It appears that CD works therapeutically by improving processes linked to sphingolipids and derivatives. The KEGG enrichment analysis of the CD-HH group showed that Coix seeds have anti-inflammatory effects by downregulating pathways such as B-cell receptor signalling, T-cell receptor signalling and Th1 and Th2 cell differentiation under high humidity (Figure 6C, D and Table 3). Inflammatory cytokine analysis found high humidity upregulated TNF-α, IL-6 and IL-17 in the HH group, but their levels were downregulated in the CD-HH group (Figure 6E–G).

Coix Seed Modulated the Humidity-Induced Inflammatory Response by Inhibiting Akkermansia spp.-Mediated Microbiome and Metabolite Dysregulation

The correlations between key microbes and metabolites in the CD-HH group under high humidity were studied (Figure 7A and B). *Ruminococcus* spp., NK4A214_group and *Prevotellaceae* NK3B31 spp. were positively correlated with SM. *Parasutterella* was positively correlated with N, N-dimethylformamide dimethyl acetal, 1,2-benzisothiazole and 2,5-dihydropyrimidine. *Akkermansia* spp. had a positive correlation with *Erysipelatoclostridium* spp. but a negative correlation with *Roseburia* spp., *Eubacterium xylanophilum* spp., *Ruminococcus* spp. and *Prevotellacea*e NK3B31 spp.

Discussion

This study explored how Coix seeds modulate the inflammatory response under high humidity, focusing on their impact on gut microbiota and metabolites. The intestinal barrier, composed of the intestinal mucosa, gut microbiota, immune system and enzymes, is a crucial defence system in the body.[17] High-humidity conditions promote pathogen growth, altering gut microbiota composition and abundance. This damages the gastrointestinal mucosa and weakens the intestinal barrier's function.[18] Pathogenic bacteria colonise the gastrointestinal mucosa, leading to diarrhoea. Subsequently, bacteria and their components cross the intestinal barrier, triggering the release of IL-6 and IL-17, which not only mediate the inflammatory response but also activate the immune system of the organism (Figure 8). The Coix seed extraction reduced the pro-inflammatory cytokines (IL-1β, TNF-α, IL-6, MCP-1) in Freund's adjuvant-induced rheumatoid arthritis rats have been reported,[19] this provides scientific evidence for Coix seed as a natural therapeutic approach for chronic inflammatory diseases.

Homeostasis in the host body depends on a balanced gut microbiota, which can be disrupted by high humidity. A higher abundance of *Erysipelatoclostridium* spp., *Proteobacteria* spp. and *Escherichia-Shigella* spp. in the HH group leads to higher TNF-α levels[20] and intestinal epithelial dysfunction.[21] *Escherichia-Shigella* spp. can better penetrate epithelial cells, causing macrophage apoptosis and IL-1β release.[22] This worsens intestinal inflammation and triggers both innate and adaptive immune responses.[23] *Akkermansia* spp. are well-known mucus degraders belonging to the phylum Verrucomicrobia.[24] High abundance of this species has been observed in mice with colonic inflammation and carcinogenic conditions.[25] *Akkermansia* spp. exhibit context-dependent roles in maintaining intestinal homeostasis, with

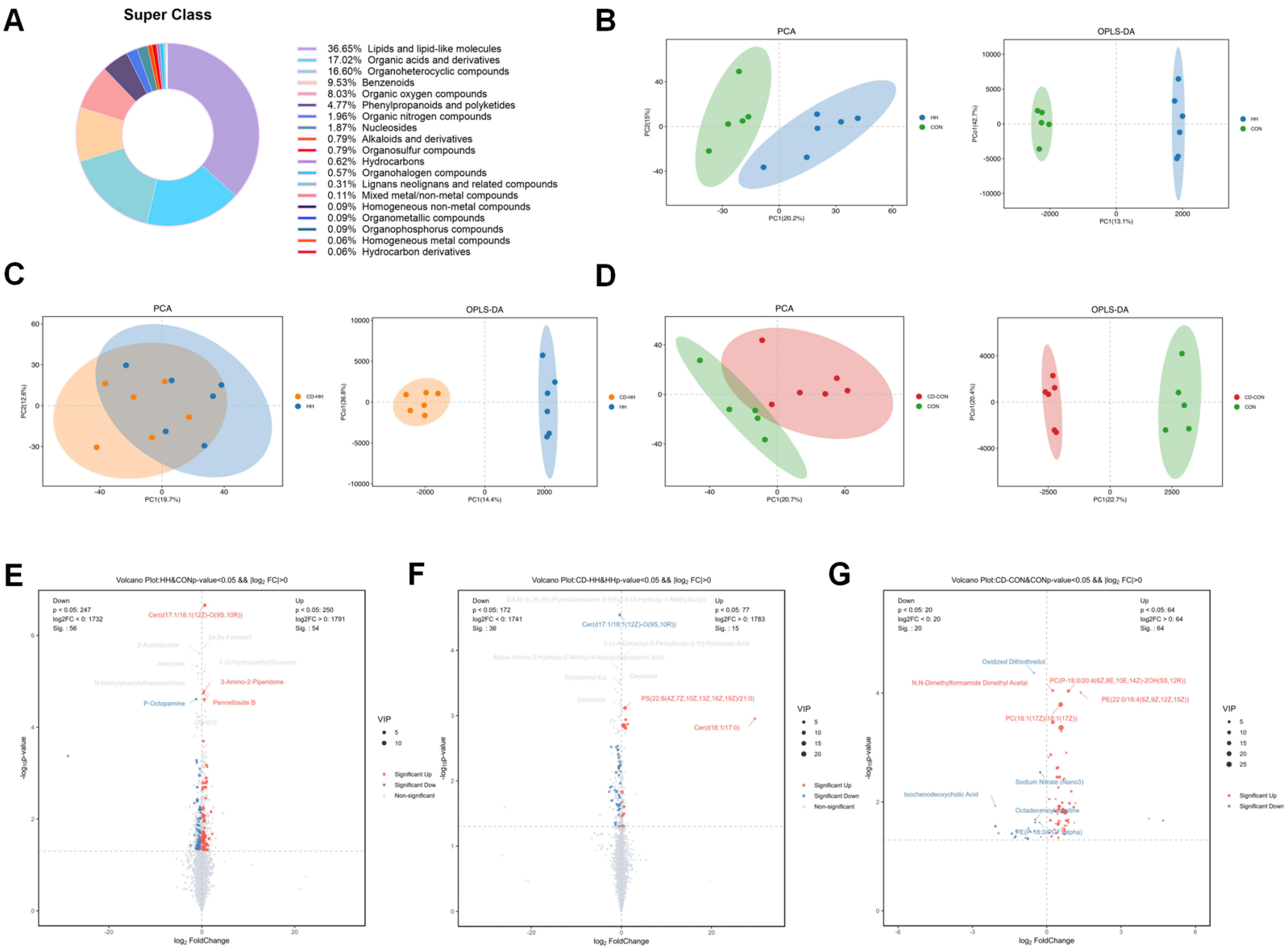

Figure 5 Different metabolites generated in HH environment. (**A**) Classification of metabolites. (**B**–**D**) PCA and OPLS-DA analyses comparing HH vs CON, CD-HH vs HH, and CD-CON vs CON, respectively. (**E**–**G**) Volcano plot of differential metabolites between CD-HH and HH, as well as CD-CON and CON groups (VIP > 1, $p < 0.05$).

Table 2 Identified Differential Metabolites Through HH vs CON and CD-HH vs HH Comparisons

No.	Metabolites	Super Class	HH vs CON				CD-HH vs HH			
			FC	VIP	P-value	Trend	FC	VIP	P-value	Trend
1	Cer(d17:1/18:1(12Z)-O(9S,10R))	Lipids and lipid-like molecules	1.58	4.61	0.000	↑	0.77	3.10	0.000	↓
2	Cer(d17:1/18:3(10,12,15)-OH(9))		1.46	2.69	0.000	↑	0.87	1.19	0.022	↓
3	SM(d18:0/22:0)		4.03	1.31	0.009	↑	0.84	2.68	0.006	↓
4	SM(d18:2/24:1)		3.33	1.36	0.011	↑	0.81	2.45	0.005	↓
5	10s,11r-Dichloro-7,11-Dimethyl -3-Methylene-4r-Hydroxy-6e,8e,12-Tridecatrienoic Acid		1.65	2.92	0.025	↑	0.63	2.61	0.004	↓
6	16,17-Dihydro-16alpha,17-Dihydroxygibberellin A4 17-Glucoside		1.98	3.96	0.035	↑	0.49	3.67	0.015	↓
7	Nigellic Acid		2.13	1.83	0.002	↑	0.61	1.11	0.028	↓
8	Phenylacetylglutamine	Organic acids and derivatives	1.73	2.86	0.023	↑	0.60	2.53	0.003	↓
9	(2s,2'S)-Pyrosaccharopine		2.33	2.25	0.0478	↑	0.45	2.03	0.007	↓
10	Stearamide		2.22	1.44	0.001	↑	0.45	1.21	0.003	↓
11	Parathion		1.77	1.75	0.003	↑	0.68	1.21	0.008	↓
12	Phosphine Oxide	Benzenoids	1.82	4.02	0.002	↑	0.68	2.79	0.006	↓
13	Demeclocycline	Phenylpropanoids and polyketides	1.37	2.41	0.047	↑	0.74	2.19	0.018	↓
14	2'-Hydroxyisoorientin		1.81	2.72	0.002	↑	0.68	1.90	0.006	↓
15	5-Methylthioribose	Organic oxygen compounds	1.67	1.33	0.046	↑	0.56	1.28	0.003	↓
16	3'-Hydroxyamobarbital	Organoheterocyclic compounds	1.51	7.71	0.038	↑	0.68	6.75	0.024	↓
17	5-Ethyl-4-Methyl-2-Pentylthiazole		1.95	2.19	0.001	↑	0.64	1.54	0.006	↓

their functional impact modulated by environmental factors.[26,27] In the current study, elevated *Akkermansia* spp. colonisation was observed in high humidity-exposed rats, correlating with subclinical inflammation activation,[28] enhanced mucolytic degradation and compromised epithelial barrier integrity – factors implicated in inflammatory bowel disease pathogenesis.[29] Mechanistic investigations suggest that *Akkermansia*-derived metabolites, including propionate, may modulate host lipid metabolism through epigenetic regulation of key metabolic mediators (eg Fiaf, Gpr43, HDACs, PPARγ) within intestinal epithelial cells.[30] Such interactions potentially drive mitochondrial bioenergetic adaptations, bile acid cycling alterations and microbiota compositional shifts.[31] Humidity-induced gut dysbiosis was further associated with disrupted bile acid homeostasis and urea nitrogen metabolism, promoting passive absorption of secondary bile acids (eg lithocholic acid) and subsequent systemic inflammation via serum cytokine elevation.[8,32] Concurrently, microbial metabolites, such as SM, Cer, stearamide and phenylacetylglutamine, demonstrated immunomodulatory effects, potentially contributing to immune dysregulation. Notably, sphingolipids – critical constituents of intestinal membrane architecture – regulate cellular apoptosis pathways and modulate natural T lymphocyte populations, suggesting their dual role in mucosal immunity and metabolic signalling.[33] Under high humidity conditions, sphingolipid metabolism may be disrupted, leading to the accumulation of specific sphingolipids and gut inflammation.[34] Sphingomyelin is an essential component of sphingolipid metabolism and is hydrolysed by alkaline sphingomyelinase

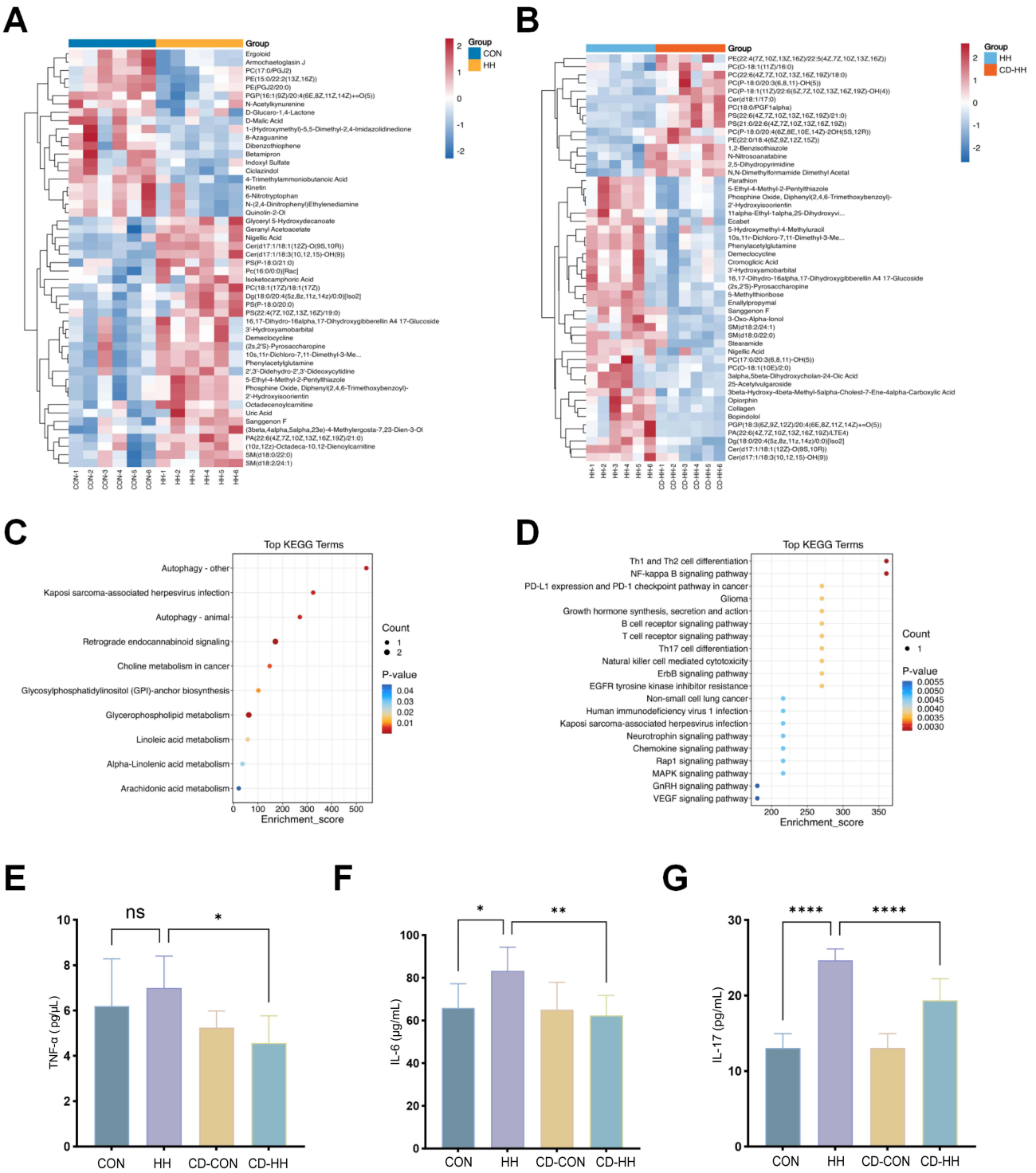

Figure 6 Metabolic pathway analysis of differential metabolites in CD-HH mice. Heatmap of hierarchical clustering analysis of metabolite differences between HH and CON groups (**A**) and CD-HH vs HH groups (**B**); (**C** and **D**) KEGG enrichment analysis of CD-HH vs HH groups; Expression levels of TNF-α expression (**E**), IL-6 (**F**), and IL-17 (**G**). Values are presented as mean ± SEM (n = 6). ns is no significance, **p < 0.01 vs CON group; *p < 0.05 vs HH group, ****p < 0.0001.

into Cer. Ceramide is a group of neurosphingolipid-reactive molecules involved in the growth, apoptosis and differentiation of intestinal cells. The conversion of SM to Cer induces mitogen-activated protein kinase pathway activation and an immune response, which further triggers apoptosis and contributes to gut inflammation.[35]

Table 3 Metabolic Pathway Analysis of CD-HH Group vs HH Group

Pathway	List Hits	Pop Hits	Enrichment Score	P-value	Substances
Glycerophospholipid metabolism	2	52	24.95	0.002	C00157, C00350
Retrograde endocannabinoid signaling	3	19	102.44	0.000	C00157, C00165, C00350
Choline metabolism in cancer	2	11	117.96	0.000	C00157, C00165
Th1 and Th2 cell differentiation	1	3	216.27	0.005	C00165
NF-kappa B signaling pathway	1	3	216.27	0.005	C00165

Coix seed, a fundamental component of TCM historically employed in managing gastrointestinal distress and systemic inflammatory disorders,[36] has emerged as a phytotherapeutic agent with a mechanistically validated capacity to regulate enteric microbial communities. Contemporary studies corroborate its prebiotic efficacy in reshaping gut microbiota composition and function, aligning empirical observations with its traditional applications in dampness-dispelling therapies. Notably, our findings extend prior evidence that Coix seeds promote probiotic growth (eg *Bifidobacterium* spp., *Lactobacillus* spp.)[37,38] and modulate circulating nitrogen,[39] which we observed in rats exposed to high humidity. This mechanism may explain Coix seed's capacity to mitigate chemically induced colonic inflammation through dual suppression of proinflammatory mediators (eg TNF-α, IL-6, IL-17) and immunoregulatory modulation.[40] Our experimental findings further substantiate this therapeutic paradigm, demonstrating Coix seed-mediated restoration of Th1/Th2 equilibrium under hyperhumid conditions – a critical immunometabolic recalibration that counteracts humidity-aggravated immune polarisation. Our work demonstrates that Coix seeds counteract humidity-specific pathogens (eg upregulation of *Erysipelatoclostridium* in the HH group) and restore sphingolipid metabolism, a pathway previously linked to humidity-agnostic inflammation but now shown to be modulated by dietary intervention in environmental stress. This nutritional–preclinical nexus underscores the unique potential of Coix seeds as humidity-resilient dietary interventions. Dietary interventions, particularly those rich in fibre, are emerging as potent modulators of gut microbiota and their anti-inflammatory metabolites.[41] Coix seeds exemplify this paradigm as a prebiotic-rich, functional food. Their nutrient-dense and health-promoting properties, including an abundance of starch, proteins, dietary fibre and vitamins,[42] have garnered significant attention. By integrating nutritional composition with microbiota–metabolite remodelling, this study positions Coix seeds as a dietary keystone for combating high-humidity environment-driven inflammatory diseases.

The present investigation revealed that dietary enrichment with Coix seed-derived fibres significantly augmented the colonisation of probiotic species, particularly *Lactobacillus* spp. and *Roseburia* spp., in rats. These observations substantiate the prebiotic capacity of Coix seeds to stimulate commensal microbial proliferation selectively, thereby counteracting humidity-mediated ecological perturbations within the intestinal ecosystem. In the HH group, Coix seed supplementation corrected microbial imbalances and metabolic disruptions, protected the mucus layer and the intestinal barrier and inhibited gut inflammation.

Limitations and Future Perspectives

This study demonstrated the noteworthy role of Coix seeds in the mitigation of gastrointestinal disorders induced by high humidity, highlighting its potential in both TCM dampness-dispelling therapy and nutritional supplementation to address extreme environmental conditions. However, the long-term effects of Coix seeds in clinical settings and their efficacy under diverse environmental conditions need to be explored in the future. This investigation was specifically designed to assess the therapeutic potential of Coix seeds in addressing humidity-induced microbial dysbiosis and metabolic dysregulation, rather than exploring dose-dependent effects. Consequently, the experimental design did not incorporate subgroup stratification for varying Coix seed dosages, focusing instead on establishing proof-of-concept for its microbiota-modulating and metabolome-restorative properties under hyperhumid conditions. Therefore, further research is required to determine the optimal dose for Coix seeds.

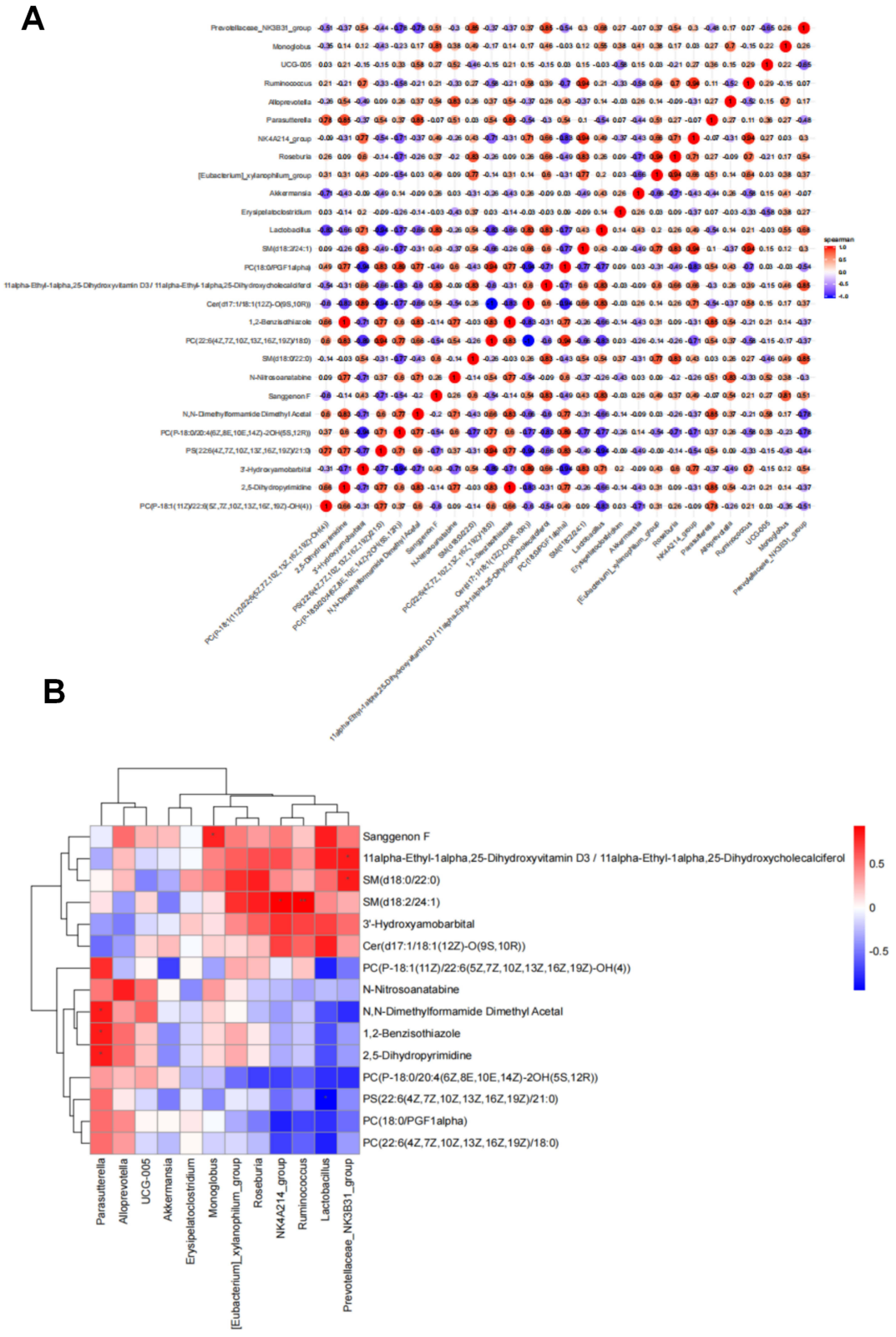

Figure 7 Association analysis of core metabolites and microbials. (**A**) Co-variation between microbes and metabolites in CD-HH group (Spearman correlation), where blue circles represent positive correlation, red circles represent negative correlation, size and shade of the circles represent the degree of correlation; (**B**) Spearman correlation heatmap of differentially expressed microflora and serum metabolites. where red color represents a positive correlation, while blue color represents a negative correlation. *p < 0.05; **p < 0.01.

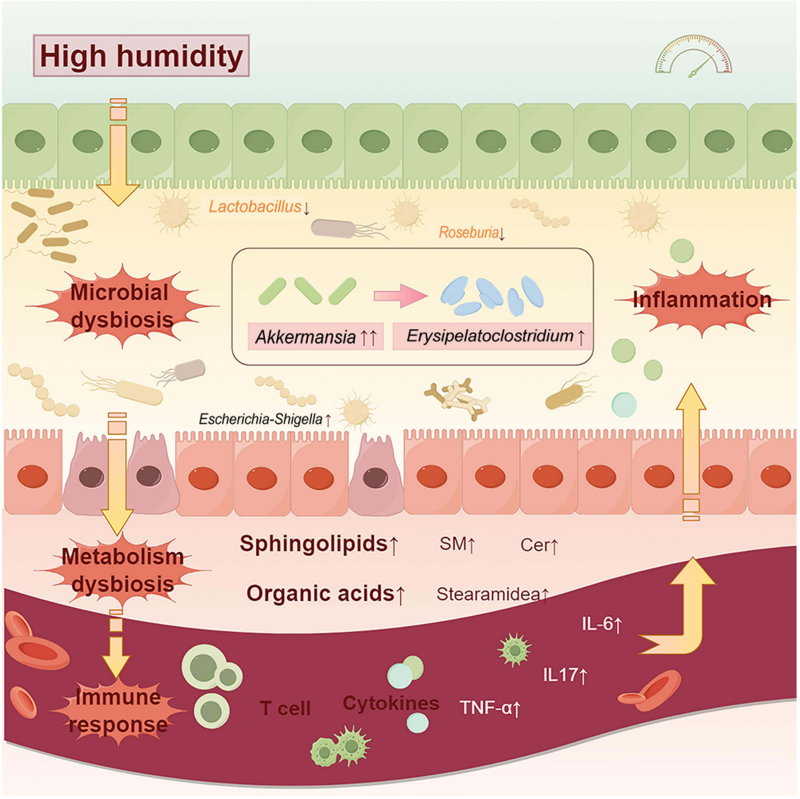

Figure 8 Schematic representation of colon inflammation in mice induced by high humidity. Under high humidity condition, higher growth of pathogens leads to changes in the composition and abundance of gut microbiota, which in turn inflicts damage to the gastrointestinal mucosa and weakens the function of intestinal barrier, bacteria and their components cross the intestinal barrier, triggering the release of IL-6 and IL-17, which not only mediate the inflammatory response but also activate the immune system of the organism.

Conclusions

The inclusion of the Ciox seeds proved to be a powerful intervention to mitigate the detrimental effects of high humidity by alleviating high humidity-induced gut dysbiosis, metabolic disorders (eg lipid metabolism disruption) and immune hyperactivation, demonstrating its potential as a novel intervention for preserving intestinal health in high-humidity environments. Given the escalating health threats from climate-driven humidity fluctuations, dietary integration of Coix seeds may serve as a sustainable strategy to enhance intestinal barrier resilience and counteract humidity-associated inflammatory cascades, which play a key role in addressing the adverse impacts of climate change on human health.

Abbreviations

WHO, World Health Organization; CD, Coix seed decoction; UHPLC-MS, Ultra-high performance liquid chromatography-mass spectrometry; SD, Sprague-Dawley; CON, control group; HH, high-humidity group; CD-CON, Coix seed decoction intervention control group; CD-HH, Coix seed decoction intervention under high-humidity; ASV, Amplicon Sequence Variant; PCA, Principle Component Analysis; PCoA, Principal Coordinate Analysis; OPLS-DA, Orthogonal Partial Least-Squares-Discriminant Analysis; LEfSe, Linear Discriminant Analysis Effect Size; VIP, Variable Importance of Projection; SM, sphingomyelin; Cer, ceramide; PS, phosphatidylserine.

Ethics Approval

All experimental procedures were conducted after taking approval from the Animal Care and Use Committee of Beijing University of Chinese Medicine (No. BUCM-2023090503-3117).

https://doi.org/10.2147/JIR.S524947

Data Sharing Statement

The data that support the findings of this study are available from the corresponding author upon reasonable request.

Acknowledgments

We would like to express our gratitude to the Research Center of Beijing University of Chinese Medicine for providing the laboratory facilities. Furthermore, we acknowledge the Shanghai Luming Biological Technology Co., LTD (Shanghai, China) for providing metabolomics services. We extend sincerest gratitude to National Natural Science Foundation of China for funding this research (NSFC, No. 8237153126); Key project at central government level: The ability establishment of sustainable use for valuable Chinese medicine resources(2060302-2301-16); The Fifth Batch of National Advanced Clinical Talent Training Program in Traditional Chinese Medicine (2022) (No. 239 [2022] of the National Administration of Traditional Chinese Medicine Human Resources and Education Department).

Funding

This research was funded by the National Natural Science Foundation of China (82374312); Key project at central government level: The ability establishment of sustainable use for valuable Chinese medicine resources(2060302-2301-16); The Fifth Batch of National Advanced Clinical Talent Training Program in Traditional Chinese Medicine (2022) (No. 239 [2022] of the National Administration of Traditional Chinese Medicine Human Resources and Education Department).

Disclosure

None of the authors have any personal, financial, commercial, or academic conflicts of interest for this work.

References

1. Raymond C, Matthews T, Horton RM. The emergence of heat and humidity too severe for human tolerance. *Sci Adv*. 2020;6:eaaw1838. doi:10.1126/sciadv.aaw1838
2. Baldwin JW, Benmarhnia T, Ebi KL, et al. Humidity's role in heat-related health outcomes: a heated debate. *Environ. Health Perspect*. 2023;131(5):55001. doi:10.1289/ehp11807
3. Filippini T, Paduano S, Veneri F, et al. Adverse human health effects of climate change: an update. *Annali di igiene*. 2024;36(3):281–291. doi:10.7416/ai.2024.2595
4. Ogden NH, Gachon P. Climate change and infectious diseases: what can we expect ? *Canada Commun Dis Rep*. 2019;45:76–80. doi:10.14745/ccdr.v45i04a01
5. Donnelly MC, Talley NJ. Effects of climate change on digestive health and preventative measures. *Gut*. 2023;72(12):2199–2201. doi:10.1136/gutjnl-2023-331187
6. Wu Y, Feng X, Li M, et al. Gut microbiota associated with appetite suppression in high-temperature and high-humidity environments. *EBioMedicine*. 2024;99:104918. doi:10.1016/j.ebiom.2023.104918
7. Wang D, Zheng Z, Yu H, et al. Impact of humid climate on rheumatoid arthritis faecal microbiome and metabolites. *Sci Rep*. 2023;13(1):16846. doi:10.1038/s41598-023-43964-4
8. Weng H, Deng L, Wang T, et al. Humid heat environment causes anxiety-like disorder via impairing gut microbiota and bile acid metabolism in mice. *Nat Commun*. 2024;15(1):5697. doi:10.1038/s41467-024-49972-w
9. Jinnouchi M, Miyahara T, Suzuki Y. Coix seed consumption affects the gut microbiota and the peripheral lymphocyte subset profiles of healthy male adults. *Nutrients*. 2021;13(11):4079. doi:10.3390/nu13114079
10. Huang DW, Wu CH, Shih CK, et al. Application of the solvent extraction technique to investigation of the anti-inflammatory activity of adlay bran. *Food Chem*. 2014;145:445–453. doi:10.1016/j.foodchem.2013.08.071
11. Yao Y, Zhu Y, Gao Y, et al. Effect of ultrasonic treatment on immunological activities of polysaccharides from adlay. *Int J Biol Macromol*. 2015;80:246–252. doi:10.1016/j.ijbiomac.2015.06.033
12. Ross FC, Patangia D, Grimaud G, et al. The interplay between diet and the gut microbiome: implications for health and disease. *Nat Rev Microbiol*. 2024;22(11):671–686. doi:10.1038/s41579-024-01068-4
13. Afshin A, Sur PJ, Fay KA. Health effects of dietary risks in 195 countries, 1990-2017: a systematic analysis for the global burden of disease study 2017. *Lancet*. 2019;393(10184):1958–1972. doi:10.1016/s0140-6736(19)30041-8
14. Peters V, Bolte L, Schuttert EM, et al. Western and carnivorous dietary patterns are associated with greater likelihood of IBD development in a large prospective population-based cohort. *J Crohn's Colitis*. 2022;16(6):931–939. doi:10.1093/ecco-jcc/jjab219
15. Han X, Ji X, Zhao H, et al. Mechanisms of coix seed compositions in the treatment of spleen deficiency and wet dampness zheng. *Afr J Tradit Complement Altern Med*. 2017;14(4):239–246. doi:10.21010/ajtcam.v14i4.26
16. Qiao B, Li X, Peng M, et al. Alteration of intestinal mucosal microbiota in mice with Chinese dampness-heat syndrom diarrhea by improper diet combined with high temperature and humidity environments. *Front Cell Infect Microbiol*. 2022;12:1096202. doi:10.3389/fcimb.2022.1096202

17. Thoo L, Noti M, Krebs P. Keep calm: the intestinal barrier at the interface of peace and war. *Cell Death Dis*. 2019;10(11):849. doi:10.1038/s41419-019-2086-z
18. Gao X, Colicino E, Shen J, et al. Impacts of air pollution, temperature, and relative humidity on leukocyte distribution: an epigenetic perspective. *Environ Int*. 2019;126:395–405. doi:10.1016/j.envint.2019.02.053
19. Li X, Zhang H, Deng Y, et al. Huaier polysaccharides inhibits hepatocellular carcinoma via gut microbiota mediated M2 macrophage polarization. *Int J Biol Macromol*. 2025;293:139357. doi:10.1016/j.ijbiomac.2024.139357
20. Chen G, Peng Y, Huang Y, et al. Fluoride induced leaky gut and bloom of erysipelatoclostridium ramosum mediate the exacerbation of obesity in high-fat-diet fed mice. *J Adv Res*. 2023;50:35–54. doi:10.1016/j.jare.2022.10.010
21. Ni J, Wu GD, Albenberg L, et al. Gut microbiota and IBD: causation or correlation? *Nat Rev Gastroenterol Hepatol*. 2017;14(10):573–584. doi:10.1038/nrgastro.2017.88
22. Yu Z, Li D, Sun H. Herba origani alleviated DSS-induced ulcerative colitis in mice through remolding gut microbiota to regulate bile acid and short-chain fatty acid metabolisms. *Biomed Pharmacothe*. 2023;161:114409. doi:10.1016/j.biopha.2023.114409
23. Litvak Y, Byndloss MX, Tsolis RM, et al. Dysbiotic proteobacteria expansion: a microbial signature of epithelial dysfunction. *Curr Opin Microbiol*. 2017;39:1–6. doi:10.1016/j.mib.2017.07.003
24. Derrien M, Vaughan EE, Plugge CM, et al. Akkermansia muciniphila gen. nov. sp. nov. a human intestinal mucin-degrading bacterium. *Intl J Sys Evolutionary Microbiol*. 2004;54(5):1469–1476. doi:10.1099/ijs.0.02873-0
25. Lang M, Baumgartner M, Rożalska A, et al. Crypt residing bacteria and proximal colonic carcinogenesis in a mouse model of lynch syndrome. *Int J Cancer*. 2020;147(8):2316–2326. doi:10.1002/ijc.33028
26. Luo Y, Lan C, Li H, et al. Rational consideration of Akkermansia muciniphila targeting intestinal health: advantages and challenges. *NPJ Biofilms Microbio*. 2022;8(1):81. doi:10.1038/s41522-022-00338-4
27. Shono Y, Docampo MD, Peled JU, et al. Increased GVHD-related mortality with broad-spectrum antibiotic use after allogeneic hematopoietic stem cell transplantation in human patients and mice. *Sci Trans Med*. 2016;8(339):339ra71. doi:10.1126/scitranslmed.aaf2311
28. Borton MA, Sabag-Daigle A, Wu J, et al. Chemical and pathogen-induced inflammation disrupt the murine intestinal microbiome. *Microbiome*. 2017;5(1):47. doi:10.1186/s40168-017-0264-8
29. Song CH, Kim N, Nam RH, et al. Changes in microbial community composition related to sex and colon cancer by Nrf2 knockout. *Front Cell Infect Microbiol*. 2021;11:636808. doi:10.3389/fcimb.2021.636808
30. Lukovac S, Belzer C, Pellis L, et al. Differential modulation by Akkermansia muciniphila and faecalibacterium prausnitzii of host peripheral lipid metabolism and histone acetylation in mouse gut organoids. *mBio*. 2014;5(4). doi:10.1128/mBio.01438-14
31. Rao Y, Kuang Z, Li C, et al. Gut Akkermansia muciniphila ameliorates metabolic dysfunction-associated fatty liver disease by regulating the metabolism of L-aspartate via gut-liver axis. *Gut Microbes*. 2021;13(1):1–19. doi:10.1080/19490976.2021.1927633
32. Yin H, Zhong Y, Wang H, et al. Short-term exposure to high relative humidity increases blood urea and influences colonic urea-nitrogen metabolism by altering the gut microbiota. *J Adv Res*. 2022;35:153–168. doi:10.1016/j.jare.2021.03.004
33. An D, Oh SF, Olszak T, et al. Sphingolipids from a symbiotic microbe regulate homeostasis of host intestinal natural killer T cells. *Cell*. 2014;156(1–2):123–133. doi:10.1016/j.cell.2013.11.042
34. Braun A, Treede I, Gotthardt D, et al. Alterations of phospholipid concentration and species composition of the intestinal mucus barrier in ulcerative colitis: a clue to pathogenesis. *Inflammatory Bowel Dis*. 2009;15(11):1705–1720. doi:10.1002/ibd.20993
35. Albeituni S, Stiban J. Roles of ceramides and other sphingolipids in immune cell function and inflammation. *Adv Exp Med Biol*. 2019;1161:169–191. doi:10.1007/978-3-030-21735-8_15
36. Ge Q, Hou CL, Rao XH, et al. In vitro fermentation characteristics of polysaccharides from coix seed and its effects on the gut microbiota. *Int J Biol Macromol*. 2024;262:129994. doi:10.1016/j.ijbiomac.2024.129994
37. Chen LC, Fan ZY, Wang HY, et al. Effect of polysaccharides from adlay seed on anti-diabetic and gut microbiota. *Food Funct*. 2019;10(7):4372–4380. doi:10.1039/c9fo00406h
38. Yang Z, Wen A, Qin L, et al. Effect of coix seed extracts on growth and metabolism of limosilactobacillus reuteri. *Foods*. 2022;11. doi:10.3390/foods11020187
39. Wang H, Yin H, Zhong Y, et al. Polysaccharides from fermented coix seed modulates circulating nitrogen and immune function by altering gut microbiota. *Curr Res Food Sci*. 2022;5:1994–2003. doi:10.1016/j.crfs.2022.10.007
40. Zhou Q, Yu R, Liu T, et al. Coix seed diet ameliorates immune function disorders in experimental colitis mice. *Nutrients*. 2021;14(1):123. doi:10.3390/nu14010123
41. Cronin P, Joyce SA, O'Toole PW, et al. Dietary fibre modulates the gut microbiota. *Nutrients*. 2021;13. doi:10.3390/nu13051655
42. Li H, Peng L, Yin F, et al. Research on Coix seed as a food and medicinal resource, it's chemical components and their pharmacological activities: a review. *J Ethnopharmacol*. 2024;319:117309. doi:10.1016/j.jep.2023.117309